Proc. of SPIE Vol. 1303, Advances in Optical Structure Systems, ed. J Breakwell, V L Genberg, G C Krumweide (Oct 1990) Copyright SPIE

Structural and optical properties for typical solid mirror shapes

Myung K. Cho and Ralph M. Richard

Optical Sciences Center
University of Arizona
Tucson, Arizona 85721

ABSTRACT

Deflections of the optical surface and optical wavefront variations of mirrors due to mechanical and thermal loads depend upon the various material and geometric design parameters. The geometric configuration of a mirror (*contour shape, total depth, edge thickness, etc.*) and material properties such as the weight density, thermal coefficients, and modulus of elasticity are required design parameters for both the earth based and spaceborne mirror applications. Mechanical properties of a mirror such as self-weight, mass moment inertia, and center of gravity are imposed geometrical design constraints. Additionally, gravitational orientations, number of support points, and support locations must be well defined. A procedure which calculates the weight, center of gravity, and areal and mass inertial properties for typical mirrors is developed. Optical surface deflections, surface quality, and fundamental natural frequency analyses of single and double arch mirror shapes for a variety of support conditions were made. Comparison of results which were obtained from the NASTRAN program and closed-form approximate solutions are presented. In addition, finite element validity and sensitivity studies were conducted to demonstrate the behavior of the element types provided in the NASTRAN program when used for optical model applications. Scaling Laws for the evaluation of the optical performances and the fundamental frequencies for geometrically similar mirrors were developed.

1. INTRODUCTION

Self-weight induced deflections and fundamental frequencies for a mirror are general design parameters of an optical system. It is often necessary to perform parametric studies in order to develop the correlations between the design parameters. Procedures to evaluate the performance of optical mirrors due to the effects of a gravity load and/or a thermal load have been developed at the Optical Sciences Center of the University of Arizona. It is the FRINGE program[1], and which is used to quantitatively evaluate the characteristics of optical surfaces from either test data or finite element analyses. The PCFRINGE[2] is a revised FRINGE program for a personal computer, and is extended to accept the output data from structural analysis programs such as NASTRAN, PAL, ANSYS, SAP IV, GIFTS, and COSMOS.

The major effort in finite element modeling is defining the geometry of the structure. A generic shape equation which can define mirror shape contours shape equation of a mirror[3] can be expressed by

$$Y = A + B\,(C - X^2)^{\frac{1}{2}} + \frac{1}{D}\,(X - E)^G + F\,X \qquad (1)$$

Parameters in Equation (1) generate circular, parabolic, linear, and combinations of these shapes for a specific mirror.

Since surface distortion over the mirror controls the qualitative performance of the optical system, for optical design purposes, the wavefront variations are required in terms of its components such as tilt, defocus, astigmatism, coma, spherical, trefoil, and other common aberrations. Program FRINGE was used to generate a least squares fit of Zernike polynomials to the deformed surface to evaluate the optical quality. Tilt and Focus terms in the optical aberrations are removed for all FRINGE analyses in this parametric design study of mirror shapes.

2. MIRROR PROPERTY ANALYSIS

Four typical solid contoured back mirror shapes (*Flat back, Double concave, Single arch, and Double arch*) were selected to investigated structural and optical properties. The evaluations of the optical performance for these contoured back shapes were discussed in reference 3; therefore, a brief discussion for the optical results is to be addressed. This current design study is mostly devoted to examining the characteristics of the fundamental frequency for the mirror shapes.

Spaceborne mirror applications require dynamic analyses of both the primary mirror and its structural support system. The support system of a proposed 40 inch primary light weight double arch mirror of the Space Infrared Telescope Facility (SIRTF), for example, must safely restrain the mirror during an emergency landing of the shuttle[4,5,6]. Additionally, the mirror itself must be strong enough to sustain a severe dynamic environment. Fundamental frequency estimations of various mirror shapes were made for equivalent height and equivalent weight contoured back mirrors at the University of Arizona[7]. Maximum structural static deflections from a 1-g load applied normal to the plane of vibration were used for a first order approximation in the study. Fundamental frequency analyses for mirrors of a variety of shapes and support systems are conducted using the NASTRAN program and an approximate closed-form solution which is given as[8]:

$$f = \frac{C}{2\pi}\left[\frac{g}{\delta_{max}}\right]^{\frac{1}{2}} \tag{2}$$

where:

f = fundamental natural frequency (Hz)
C = correction factor (=1.277)
g = acceleration due to gravity
δ_{max} = maximum static deflection

Since well-known solutions[9,10,11] exist for a flat circular plate with a uniform thickness, the following mirror shapes with non-uniform thickness were considered to evaluate the fundamental frequencies: (1) double concave mirror shapes, (2) single arch mirror shapes, and (3) double arch mirror shapes.

Fundamental frequencies depend upon the support conditions; therefore, the followings were used in this parametric design study: (1) a RING, a six at 60 degrees (6-60), or a three at 120 degrees (3-120) support system for every mirror configuration with (2) support point ratios ranging from 0.50 through 0.70 for the double arch mirror shapes.

For this parametric design study, each mirror has a 40 inch in diameter supported in the ZENITH position (optical axis vertical) and made out of SXA, an aluminum and silicon carbide metal matrix composite. SXA has the following material properties:

Elastic modulus = 16.0×10^6 psi
Poisson's ratio = 0.30
Weight density = 0.10 lb/in^3

2.1. Flat back mirror

A 40 inch diameter f/2.0 flat back mirror model is shown in Figure 1, in which only the half of the entire mirror cross section was used for illustrative purposes. This mirror shape, which weighs 545 pounds, is used as a "baseline", and the surface deformations were evaluated. Maximum structural surface deflections for various support ratios are listed in Table 1. Shown in Figure 2 is the surface deflection versus the support ratio for each support system. The least amount of structural deflection occurs when this mirror is supported at 0.7 radius for all support system.

Given in Table 2 and Figure 3 is the optical surface RMS (the square Root of the Mean Squares) wavefront variation versus the support ratio for the support systems. When a mirror was supported by a RING at r/Ro=0.1, for example, the RMS wavefront error of the optical surface was 0.630 waves (λ = 6,330 angstroms, 0.6328 micro meters, or 25 micro inches). For this particular shape of mirror, the lowest RMS wavefront error results when either the ring support or 12-30 support system is at about 0.6 radius. If the 3-120 support system is a design requirement, then the optical structure needs to be supported at about 0.5 radius to get the optimum optical performance. Through these analyses it is found that the optimum support location depends on the support systems, and the support ratio lies between 0.5 and 0.6 for all the flat back mirrors.

2.2. Double concave mirror

An attribute of double concave mirror shapes is the symmetry of the optical and the back surfaces. This geometric feature ensures that the structural plane of symmetry and the center of gravity are coincident. Therefore, it generally is the best for mirrors used in a HORIZON application[3]. A 40 inch f/2 SXA mirror with both the optical and back surfaces concave and supported at the outer edge (r/Ro=1.0) was analyzed. This mirror has a radius of curvature of 160 inches for the front and back surfaces with an outer edge thickness of 5.0 inches and an inner edge thickness of 2.6 inches. This mirror was labelled as configuration 1 and is shown in Figure 4. Evaluation of the optical performance for this configuration was made for various boundary conditions. In order to examine the effect of the thickness of the mirror, another configuration with an outer edge thickness of 4.0 inches and an inner edge thickness of 1.6 inches, labelled as configuration 2 as shown in Figure 5, was analyzed as well.

Listed in Table 3 are the first three natural frequencies for both the two mirror configurations supported by a RING, a six point support (6-60), and a three point support (3-120), respectively. The fundamental mode shape for configuration 1 supported by 6-60 are shown in Figure 6. In this figure, only the top layer of elements of the mirror model was used illustration. The first mode shape which is a pure vertical motion is at 470 Hz. The second mode, which is a mixed torsional vertical translation, occurred at 1850 Hz[12].

A summary of the structural and optical results for both configurations is listed in Table 4. The fundamental frequencies, obtained from NASTRAN models for a ring support, were 492 Hz for mirror configuration 1 and 360 Hz for configuration 2. For a 6-60 support system, the fundamental frequency as well as the maximum surface deflection were very close to that for a RING support. The natural frequencies for these configurations, supported by a 3-120 system, were estimated as 362 Hz and 281 Hz, respectively.

The closed-form solution has successfully predicted the fundamental frequencies of these double concave mirrors, with variety of boundary conditions, to within seven percent of the NASTRAN results. The estimates did not predict, however, a lower bound or an upper bound of the NASTRAN results. This implies that it may not be easy to specifically determine the correction factor 'C' in Equation (2) for this mirror shape.

2.3. Single arch mirror analyses and designs

A 40 inch single arch SXA mirror with a maximum depth of 5.0 inches was optimally designed for minimum weight and analyzed. As shown in Figure 7, the mirror has a 4.0 inch diameter central hole, an outer edge thickness of 0.5 inches, and a 2.0 inch land. The self-weight was 135 pounds and it was supported at r/Ro=0.15 (Configuration 1). Another single arch shape of the same configuration with the exception of the size of the land with r/Ro=0.20 was also optimally designed and analyzed (Configuration 2 as shown in Figure 8).

Listed in Table 5 are the first three natural frequencies for both the two mirror configurations supported by a RING, a 6-60, and a 3-120 system, respectively. A comparison between the two configurations was made and listed in Table 6. For a RING support, the fundamental frequency was estimated as 435 Hz for configuration 1, and as 556 Hz for configuration 2. The optical RMS wavefront error was 0.175 λ for configuration 1, and for configuration 2 the RMS was approximately 30 percent greater. A comparison of the results for these specific mirrors supported by a RING, a 6-60, and a

3-120 support system, shows that for all practical purposes the mirror performances are identical to one another statically, optically and dynamically. Good correlation between the results from NASTRAN and the closed-form solution was apparent. For this mirror shape, the closed-form solutions agreed with the NASTRAN results to within six percent. The conclusion can be drawn that for this 40 inch f/2 single arch mirror the structural and the optical properties are practically identical regardless of the support conditions.

2.4. Double arch mirror designs

Four typical 40 inch f/2 SXA double arch mirrors with various support conditions were considered. Each has a distinctive back contour, but all have the same inner edge thickness of 0.5 inches and outer edge of 0.5 inches. The 0.5 inch minimum thickness of the edge was a optical shop constraint. Making mirrors of these sizes with thinner edges is not practical. The radius of curvature is 160 inches for all mirrors. Typical cross sections of the basic shapes and the parameters of each back contour, defined by Equation (1), are shown in Figure 9. A typical finite element model for a 40 inch double arch mirror is shown in Figure 10. The finite element model is comprised of 1548 solid elements and 1862 grid points for a total of 5586 total degrees of freedom. The NASTRAN computer access time on the CYBER 175 at the University of Arizona was estimated as 3780 CPU seconds and 10972 system seconds.

The evaluation of the optical surface performance in terms of RMS wavefront errors were listed in reference 3, which showed that the RMS wavefront error value is strongly dependent upon both the contour back shape and support system. Fundamental frequency analyses were performed for the same contoured back shapes. In order to examine the validity of the closed-form solution for a double arch mirror shape, mirrors of various contoured back shape equations with support ratio ranging from 0.5 to 0.7 were used. Each mirror configuration was supported by a different number of support points.

Listed in the Table 7 is a summary of the results for double arch mirror shapes with the contoured back equation of (EQN 2-3) for various support conditions. The fundamental frequencies obtained from NASTRAN were well bounded to within ten percent of a maximum difference for the various support conditions. When the mirror with (EQN 2-3) contoured back shape, for example, is supported by a RING at r/Ro=0.50, the fundamental natural frequency is 1080 Hz. For a 3-120 at the same support location for the same shape, a lower frequency at 930 Hz is found. The stiffest model in a dynamic sense was a mirror supported by a RING at r/Ro=0.60, here the smallest surface deflection can be found as well.

The estimations by the closed-form did not correlate to those from NASTRAN for every configuration. For a support ratio r/Ro=0.5, however, the estimations appeared to be in reasonably good agreement. The reason for this is that the frequency responses are commonly associated several other features of a mirror configuration rather than the maximum surface deflection alone which is the only parameter used in the closed-form solution. Hence, the closed-form estimation may not be applicable to these double arch mirror shape.

For a further verification of the use of the closed-form solution in the case of r/Ro=0.5, additional models were made with the contoured back equations of (EQN 4-5) and (EQN 6-7). The results obtained from these three contoured back shapes supported by a RING at r/Ro=0.5 were summarized in Table 8. A maximum 15 percent difference was observed between the two methods. Hence, the closed-form solution may be adopted as a good first order approximation to these mirror shapes supported at a 0.50 radius for different support systems.

In order to integrate the ideas of the effects of support conditions in the estimation of fundamental frequencies, a frequency ratio was used, as shown in Table 9, where the frequency ratios for a 6-60 and a 3-120 to a RING support system are listed. For example, fundamental natural frequencies of 6-60 supported mirrors are about 97 percent of those for RING supported mirrors of identical shape. For a double concave mirror supported by a 3-120, the fundamental frequency may be estimated as about 75 percent of that for a RING. Similarly, the fundamental frequency of a three point supported single arch is 95 percent of that for a RING. For double arch mirror shapes, the ratio is about 85 percent. This implies that a great saving in effort is possible during input data preparation and the computer access time. A mirror with a RING support can be modeled as an axisymmetric model; therefore, at least one order of magnitude of the computer access time can be reduced compared to the analysis for a 3-120.

3. FINITE ELEMENT MODELING STUDY

In this section some of the finite element modeling technique and its application to mirrors are described, and some numerical results are presented. The finite element method is an analysis technique which divides a structure with a finite number of elements and, in general, finer element mesh sizes result in improved accuracy of solution (convergence theorem). Additionally, the accuracy and performance of the structural model depends on the different elements used. A mirror modeled with plate elements, for example, will produce different displacement fields over the structure depending on the use of various kinds of elements such as elements with only membrane, elements with membrane and bending with or without coupling, elements with shear or without shear deformation capability. Herein element validity and sensitivity studies are performed to ensure that the element types provided in the NASTRAN program are properly used. For a finite element modeling study, the following three different structural models are examined: (1) uniform flat back mirror models, and (2) contoured back mirror models.

3.1. Uniform flat back mirror models

A flat mirror with a constant thickness is modeled using various aspect ratios, D/t (ratio of the diameter of a mirror to the depth). In general, plates with a uniform thickness are classified by the aspect ratio. For plates with an aspect ratio of about 17 or larger, the thin plate theory (Kirchhoff plate theory) which does not account for the shear effect can be applied. For a smaller aspect ratio, the thick plate theory (Mindlin plate theory) which takes shear effects into account should be applied. Assumptions behind the theories are well known and easily found in several references 13 and 14.

A study of a 40 inch flat primary mirror was performed to investigate the effects of the self-weight induced deflections over the optical surface for various aspect ratios. A typical mirror configuration simply supported at the outer edge is shown in Figure 11. Five different aspect ratios ranging from 4 through 25 were considered, and each was analyzed for the following three different support systems: (1) a RING support, (2) a six equally spaced supports at 60 degrees (6-60), and (3) a three equally spaced supports at 120 degrees (3-120). The mirror was modeled for each support system by: (1) a plate bending element without shear capability, (2) a plate bending element with shear, and (3) solid elements using four layers. For the RING support, an axisymmetric NASTRAN model was utilized to compare the performance to the other models with different element types. Results from closed form solutions without shear and from the NASTRAN program for each case are listed in Table 10.

Since the theoretical approach did not include shear deformation, it correlated most closely to the results of the plate model without shear. As expected, a plate model without shear is stiffer than that with shear. The shear effect in these plate models does not seem to be significant for a RING support system, but it increases with a fewer number of support points. For a relatively thin mirror, the results obtained from the solid and the plate models with shear effect are in good agreement for each support system. An excellent correlation was found between the results of the axisymmetric and the solid models for a RING support system. It is notable that an axisymmetric mirror model may be quite applicable to a mirror supported by a RING in that this model requires the smallest amount of effort in preparation of the input data and the shortest CPU access time in the analysis.

For mirror models with aspect ratios of 25 (D/t=25), the overall differences in the maximum deflections between the plates with shear and without shear deformation were less than four percent. In this case the shear term was small; therefore, it may be neglected (Thin Plate Theory). A two percent difference is observed between a plate model with shear and a solid model. In the case of D/t=16, a maximum difference of ten percent was found between both plate models supported by a RING. The results obtained from both the solid and the plate models were in good agreement for each support system. For a thick mirror the differences become apparent because shear deformation is now significant. A maximum 23 percent difference was observed between solid and plate models supported by a (3-120) for D/t=8. The thickest mirror model, D/t=4, yielded results which were very different from one another. The plate model (shear included version) predicted the maximum deflection about three times lower than the solid model for the case of a three point support system. Hence, even a plate model which has shear capability is not valid for thick mirror analyses. Similar observations have been made by Maser, et al.[15], and Ditolla, et al.[16].

3.2. Contoured back mirror models

Minimizing the self-weight induced deflections of a mirror by reducing its self-weight has led to the concept of the light weight mirror designs. There is no closed form solution for the deflections on the optical surface for arbitrary contoured back mirror shapes. Hence, finite element applications to these mirror shapes must be treated with great care. Orringer and Tong[17] presented the uses and abuses of the finite element method for several structural applications.

In order to verify the validity of a plate model for a contoured back mirror application, 40 inch SXA single arch and double arch mirrors, were used. Each mirror shape has a flat optical surface and does not have the central hole. Shown in Figure 12 is the cross section of the single arch mirror configuration. This mirror was modeled such that the plane of the geometric center of the mirror represents the mid-plane of the plate model. Additionally, a cross section of the double arch mirror and the mid plane of its plate model are shown in Figure 13. A comparison of the maximum structural deflection was made between the plate model with shear deformation, the solid model, and the axisymmetric model for each mirror configuration. The results obtained from these models for a RING, a (6-60), and a (3-120) support are listed in Table 11. For the single arch mirror configuration a maximum difference of 35 percent was observed, whereas a 15 percent difference was found for the double arch mirror configuration. Very good correlation was also obtained between the double arch models supported by either a 6-60 or a 3-120.

Evaluations of the optical performance were made and listed in Table 12. During this evaluation process, for the plate model, the geometry data over the optical surface was assumed to be the same as the solid model. The RMS errors obtained from the plate model of the single arch are six times higher than that of the solid model. It may be interpreted that for the plate model the deflection at the support point is zero whereas it is not zero for the solid model. Therefore, a sharp discontinuity exists over the optical surface in the plate model which causes a significant effect in evaluation of the optical performance. For the double arch mirror configuration, the plate model has an RMS wavefront variation three times higher than the solid model. It is apparent that using the appropriate finite element model for each application is important. A plate model for a contoured back mirror application may misinterpret the significant mechanical characteristics of the actual mirror. This model may be totally unacceptable when it is used for the evaluation of the optical performance.

4. SUMMARY AND CONCLUSIONS

A parametric study for structural and optical properties of solid contoured back mirrors has been presented. The NASTRAN program was used primarily to estimate structural performances of mirrors, and the FRINGE program was used to evaluate the optical performances. Through examining various contoured back shapes based on the imposed design constraints, the following conclusions were drawn:

(1) The structural and optical performances were very sensitive to the material parameters, contoured back shape, and support location.

(2) For the baseline mirror configuration (*40 inch flat back*), the optimal support location for structural surface deflection was 0.7 radius regardless of number of support points. The lowest RMS wavefront variation occurred when supported by a RING at r/Ro=0.60. The optimum support point location tended to move inward to the optical axis as a number of support points decreased. For a 3-120 support system, the baseline configuration supported at r/Ro=0.50 performed best in an optical sense.

(3) The optical performances for the 40 inch single arch mirror shapes were practically identical regardless of the support systems.

(4) The approximate closed-form solution successfully predicted the fundamental natural frequencies of the double concave and single arch mirror shapes for a variety of boundary conditions. For the double arch mirrors, however, this closed-form estimation is not applicable.

(5) RMS variations and fundamental frequencies of all 40 inch f/2 mirror configurations supported by a 6-60 were practically identical to those supported by a RING.

(6) The plate model with shear in the NASTRAN program library performed adequately for high values of the aspect ratio (D/t), but the model seemed to be considerably stiffer than the solid model

for low values of the aspect ratios. The plate models for a contoured back mirror may not represent the significant mechanical characteristics of the actual optical system or mirror. In the case of the evaluation of the optical performance, the plate model for a contoured shape application may be totally unacceptable.
(7) This study used a SXA 40 inches mirror for all structural and optical properties. Generic scaling laws[12] can be utilized for the mirror which has a geometric similarity and/or different material properties in order to the evaluate the optical performances and the fundamental frequencies as:

$$RMS = \left[\frac{\rho}{\rho_{ref}}\right]\left[\frac{E_{ref}}{E}\right]\left[\frac{A}{A_{ref}}\right] RMS_{ref}$$

where A stands for the cross sectional area of a mirror, and the subscript of "ref" in this equation represent the values or parameters associated with the reference mirror configuration, and

$$f = \left[\frac{\rho_{ref}}{\rho}\right]^{\frac{1}{2}}\left[\frac{E}{E_{ref}}\right]^{\frac{1}{2}}\left[\frac{D_{ref}}{D}\right] f_{ref}$$

where f is the fundamental frequency, D stands for the diameter of a mirror.

5. ACKNOWLEDGEMENT

This Study was partially supported by NASA Ames Research Center through the NASA Cooperative Agreement NAG2-426 with the University of Arizona. The authors wish to acknowledge Ramsey Melugin of the technical staff at NASA Ames for his helpful suggestions.

6. REFERENCES

1. Anderson, D., *FRINGE Manual*, Version 3, Optical Sciences Center, University of Arizona, Tucson, Arizona, April 1982.
2. Cho, M. K. and Richard, R. M., *PCFRINGE - An Optical Performance Program Using Structural Deflections*, University of Arizona, Tucson, Arizona, 1989.
3. Cho, M. K., Richard, R. M., and Vukobratovich, D., *Optical Mirror Shapes and Supports for Light Weight Mirrors Subjected to Self-weight*, SPIE - the International Society for Optical Engineering, Vol. 1167, 1989.
4. Richard, R. M., Vukobratovich, D., Pollard, L. W., and Cho, M. K., *SIRTF Primary Mirror Mount Flexure and Socket Design*, NASA Ames Research Center, Mail Stop 244-7, Moffett Field, California 94035, 1988.
5. Richard, R. M., Vukobratovich, D., Cho, M. K., and Pollard, L. W., *The Flexure Assembly Design for the SIRTF One-Meter Primary Mirror*, Proceedings of SPIE - the International Society for Optical Engineering, Vol 973, 1988.
6. Richard, R. M., Cho, M. K., and Pollard, L. W., *Dynamic Analysis of the SIRTF One-Meter Mirror During Launch*, Proceedings of SPIE - the International Society for Optical Engineering, Vol 973, 1988.
7. Richard, R. M., Vukobratovich, D., Valente, T. M., and Cho, M. K., *Interim SIRTF Primary Mirror Parametric Study*, NASA Ames Research Center, Mail Stop 244-7, Moffett Field, California 94035, 1989.
8. Blevins, R. D., *Formulas for Natural Frequency and Mode Shape*, Van Nostrand Reinhold Company, 1979.

9. Roark, R. J., *Formulas for stress and Strain*, 5th Edition, Mcgraw-Hill, New York, 1975.
10. Ugural, A. C., *Stresses in Plates and Shells*, McGraw-Hill, 1981.
11. Lekhnitskii, S. G., Tsai, S. W., and Cheron, T., *Anisotropic Plates*, Gordon and Breach Science Publishers, 1968.
12. Cho, M. K., *Structural Deflections and Optical Performances of Light Weight Mirrors*, Ph. D. Dissertation, University of Arizona, Tucson, Arizona, 1989.
13. Timoshenko, S. P. and Woinowsky-Kreiger, S., *Theory of Plates and Shells*, Mcgraw-Hill, 1959.
14. Selke, L. A., *Theoretical Elastic Deflections of a Thick Horizontal Circular Mirror on a Ring Support*, Applied Optics, Vol. 9, No. 1, January 1970.
15. Maser, K. R. and Soosaar, K., *Elastic Analysis of Large Spacebound Mirrors*, Space Optics - Proceedings of the Ninth International Congress of the International Commission for Optics, Santa Monica, California, 1982.
16. DiTolla, R., Richard, R. M., and Vukobratovich, D., *Design of a Support System for the Primary Mirror of a Cryogenic Space Telescope*, SPIE - the International Society for Optical Engineering, Vol. 619, 1986.
17. Orringer, O. and Ting, P., *Uses and Abuses of the Finite Element Method*, Proceedings of SPIE - the International Society for Optical Engineering, Vol. 450, 1984.

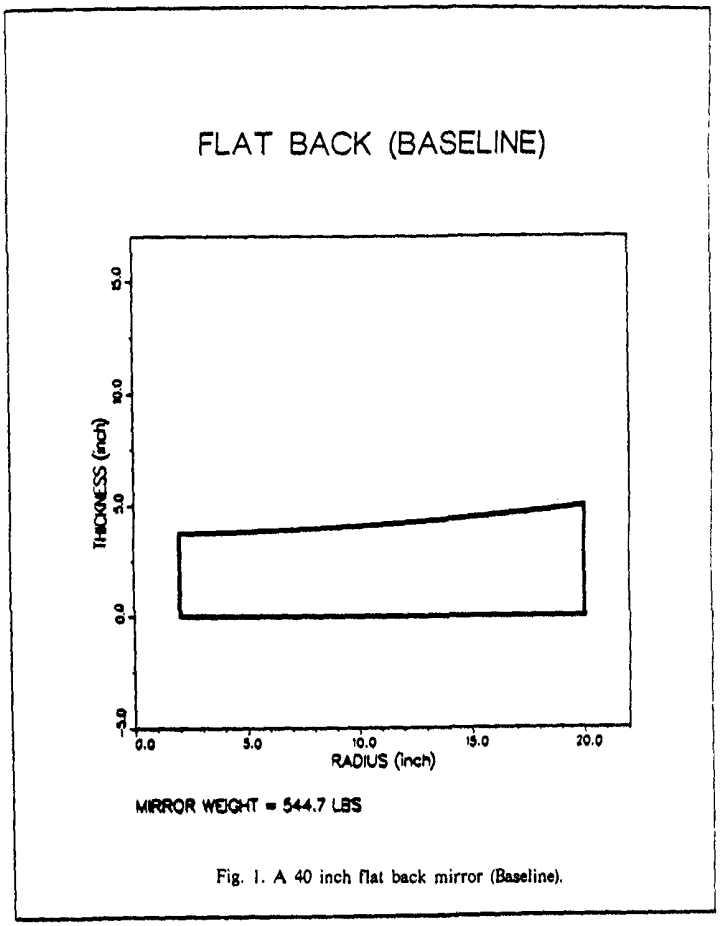

Fig. 1. A 40 inch flat back mirror (Baseline).

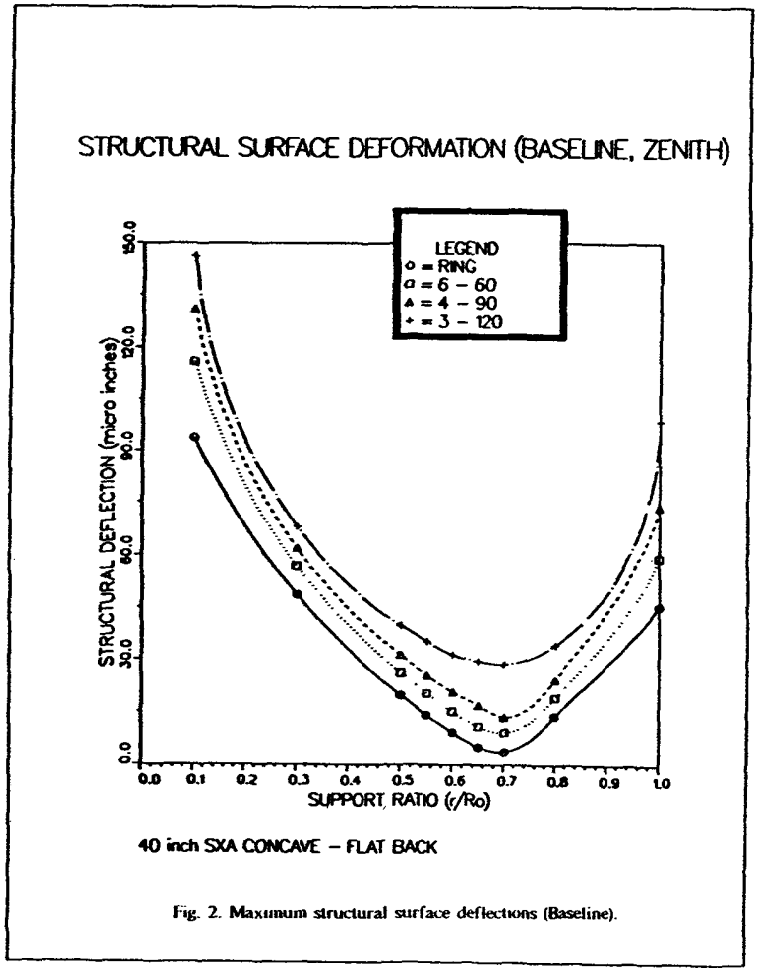

Fig. 2. Maximum structural surface deflections (Baseline).

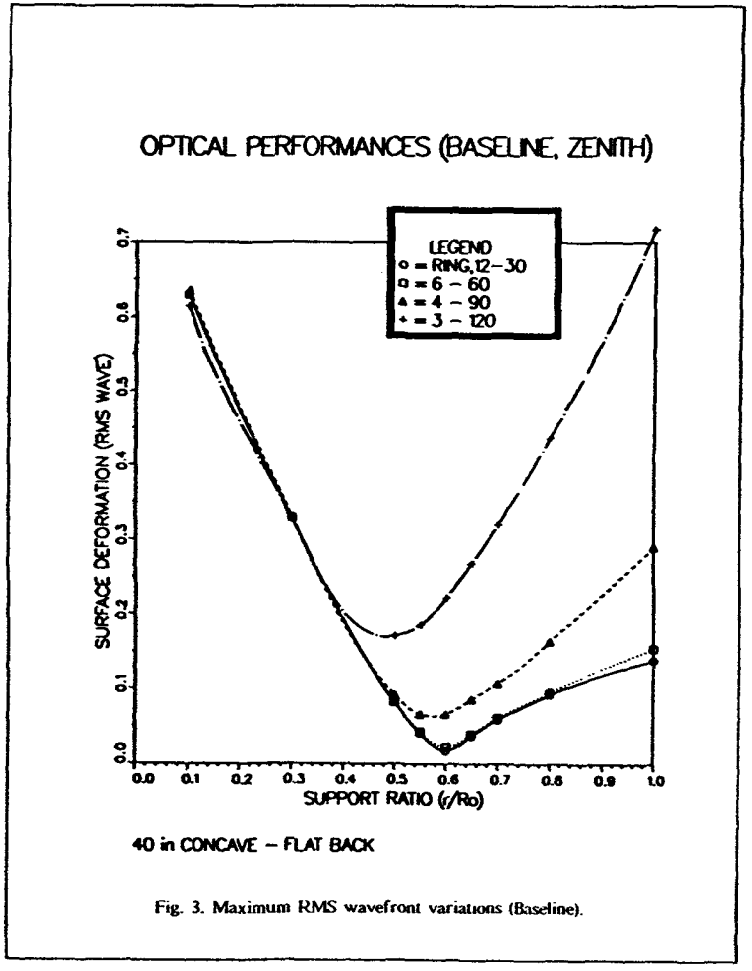

Fig. 3. Maximum RMS wavefront variations (Baseline).

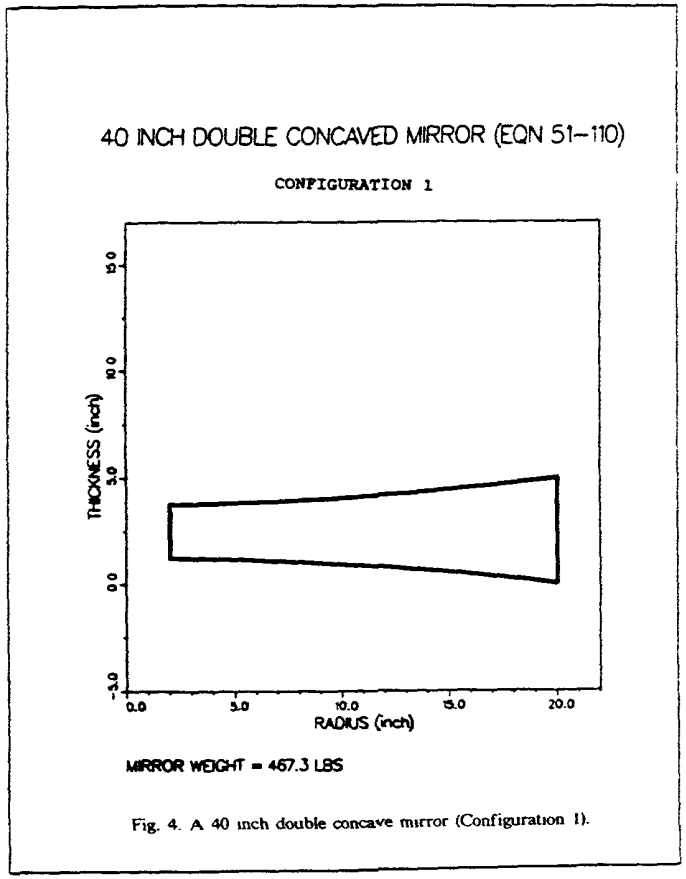

Fig. 4. A 40 inch double concave mirror (Configuration 1).

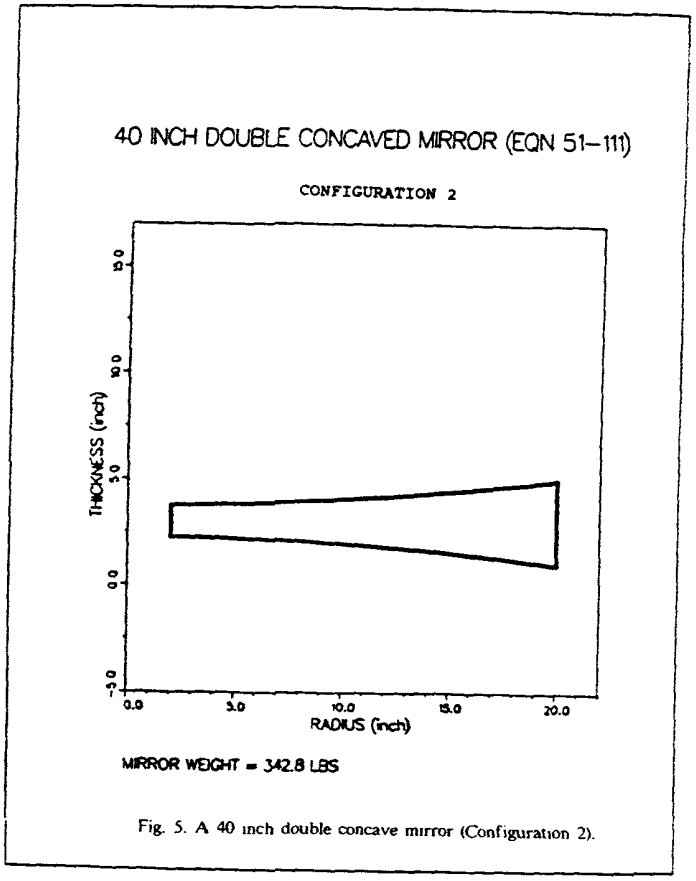

Fig. 5. A 40 inch double concave mirror (Configuration 2).

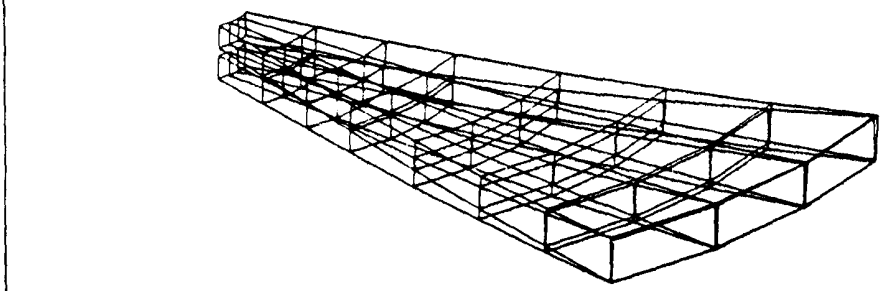

Isometric View

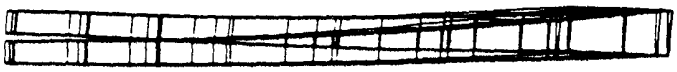

Elevation View

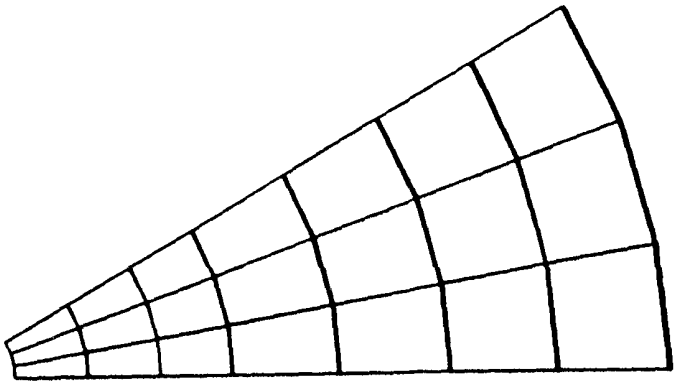

Plan View

Fig. 6. Frequency mode 1 at 470 Hz for Configuration 1 (6-60 support).

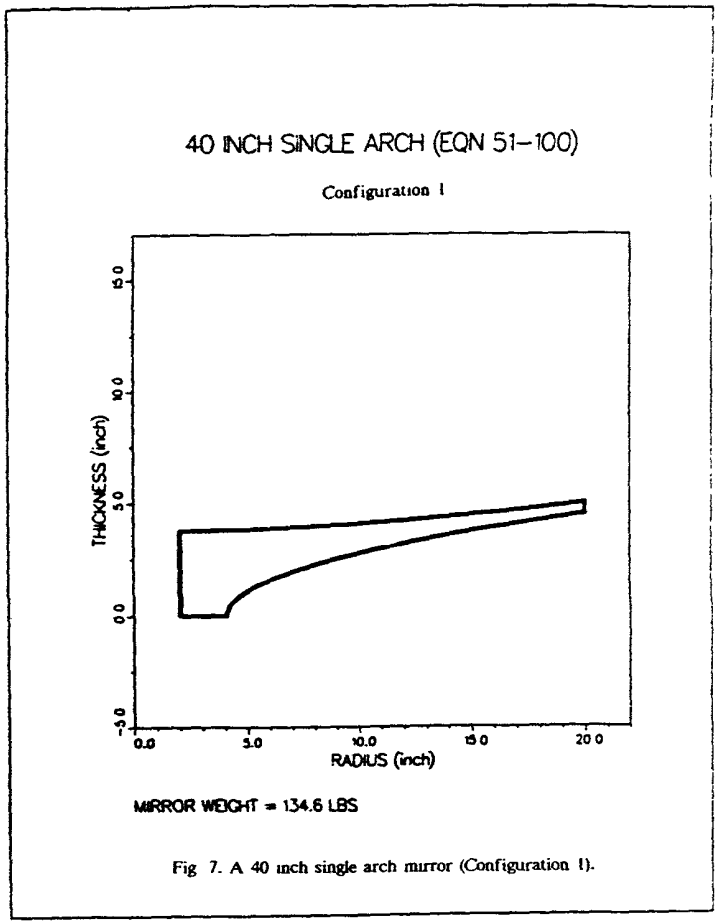

Fig. 7. A 40 inch single arch mirror (Configuration 1).

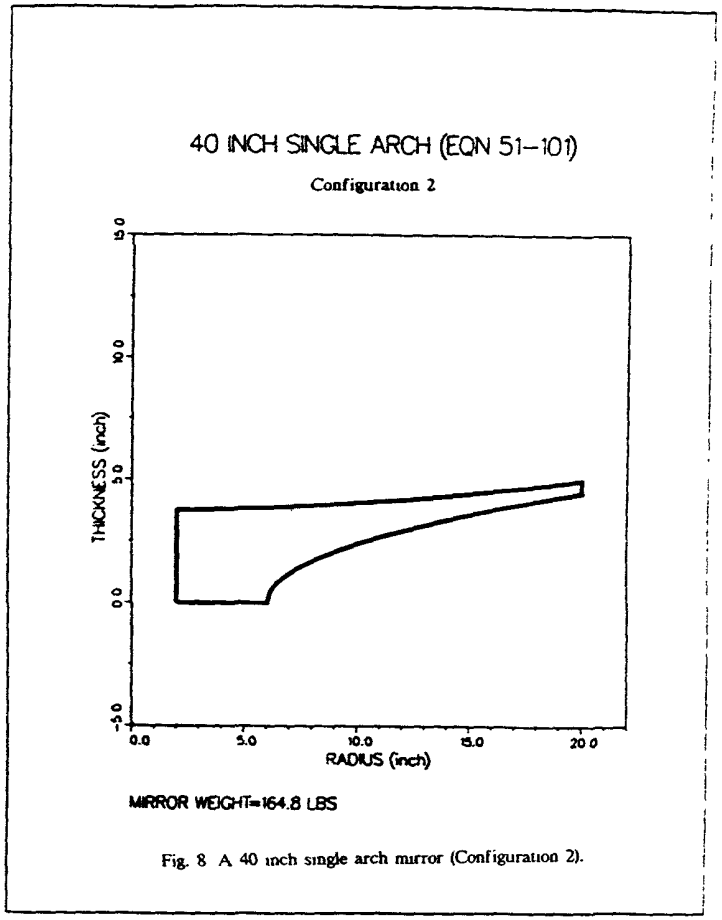

Fig. 8. A 40 inch single arch mirror (Configuration 2).

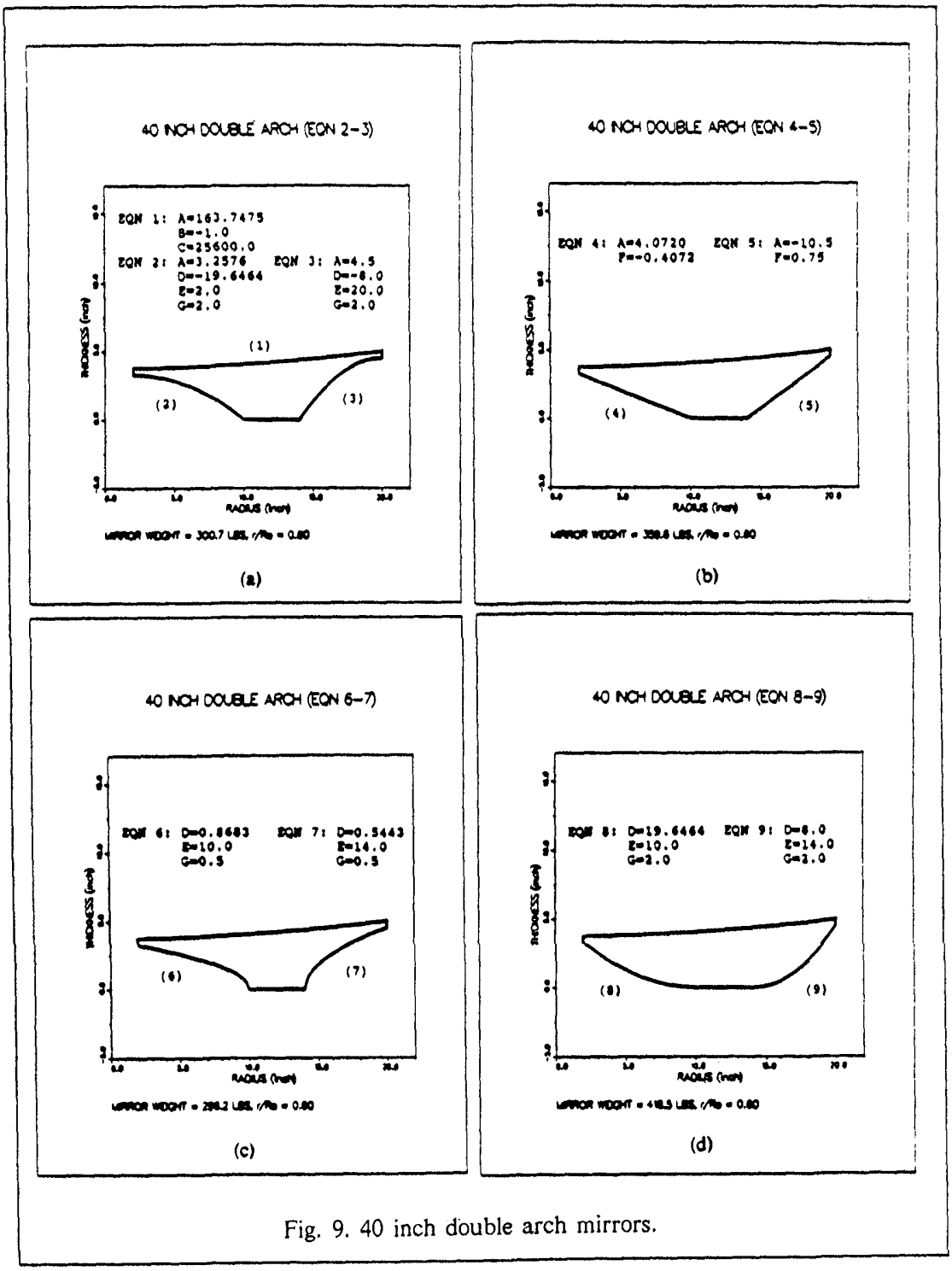

Fig. 9. 40 inch double arch mirrors.

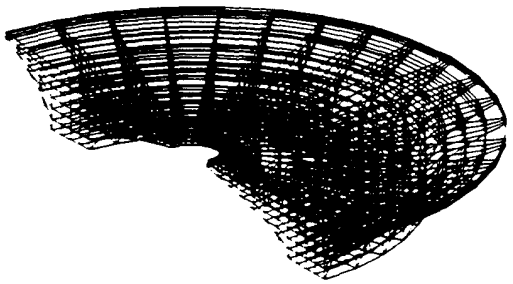

Fig. 10. Typical finite element model supported at r/Ro=0.65.

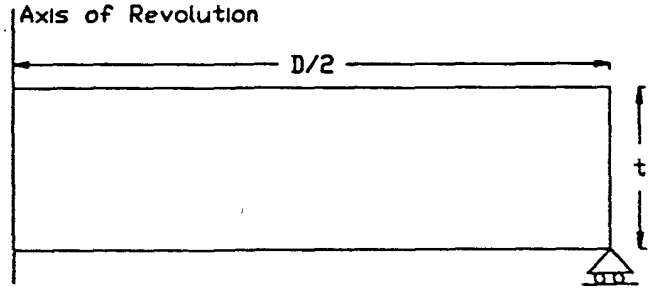

Fig. 11. A uniform flat back mirror model.

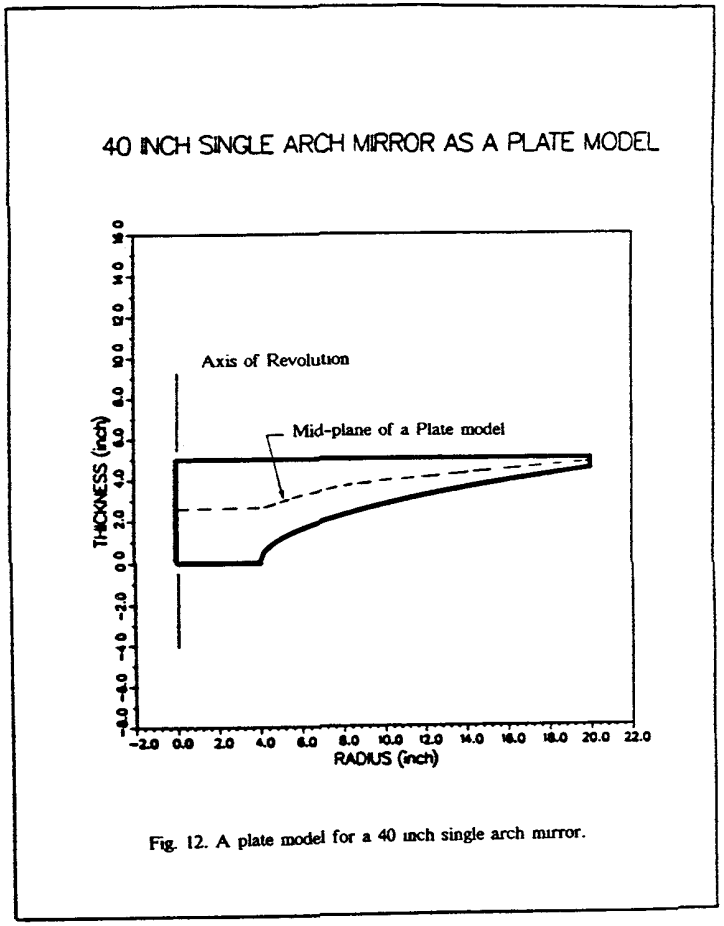

Fig. 12. A plate model for a 40 inch single arch mirror.

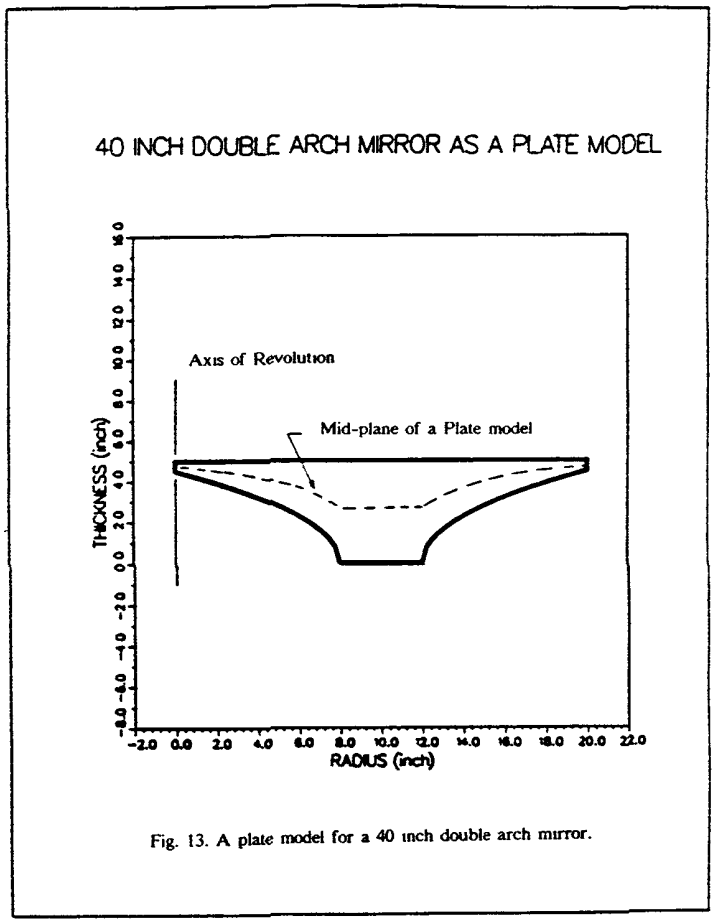

Fig. 13. A plate model for a 40 inch double arch mirror.

Table 1. Maximum Structural Deflection of Flat Back Mirror (Baseline)
(40 inch F/2 SXA Solid Mirror)

SUPPORT r/Ro	GRAVITY LOAD	SURFACE DEFORMATION (micro in.) RING	6-60	4-90	3-120
0.10	ZENITH	93.75	115.94	130.91	146.32
0.30	ZENITH	48.74	56.82	62.00	68.22
0.50	ZENITH	19.80	26.30	31.32	39.80
0.55	ZENITH	14.09	20.34	25.59	35.19
0.60	ZENITH	9.08	15.15	20.75	31.32
0.65	ZENITH	4.83	10.79	16.88	29.51
0.70	ZENITH	3.53	9.05	13.53	28.67
0.80	ZENITH	13.83	19.15	24.41	34.28
1.00	ZENITH	45.57	59.38	73.93	98.81

Table 2. 40 inch SXA mirror baseline (Concave-Flat)

SUPPORT r/Ro	GRAVITY LOAD	---- SURFACE DEFORMATION (RMS WAVE) ---- RING	12-30	6-60	4-90	3-120
0.10	ZENITH	0.630	0.630	0.631	0.637	0.620
0.30	ZENITH	0.328	0.328	0.329	0.330	0.326
0.50	ZENITH	0.082	0.082	0.084	0.091	0.171
0.55	ZENITH	0.040	0.041	0.042	0.066	0.186
0.60	ZENITH	0.017	0.018	0.022	0.066	0.222
0.65	ZENITH	0.036	0.037	0.039	0.086	0.268
0.70	ZENITH	0.058	0.059	0.061	0.107	0.320
0.80	ZENITH	0.092	0.093	0.096	0.164	0.437
1.00	ZENITH	0.138	0.140	0.154	0.290	0.717
--	HORIZON	0.028	0.028	0.029	0.030	0.045

Table 3. The First Three Lowest Natural Frequencies for
40 inch Double Concave Mirrors

	Mode	RING	6-60	3-120
Double Concave (Configuration 1)	1	492 Hz	470 Hz	362 Hz
	2	2640	1850	930
	3	5730	3380	2480
Double Concave (Configuration 2)	1	360 Hz	350 Hz	281 Hz
	2	1920	1530	690
	3	4420	2560	1990

Table 4. A Comparison Summary of Double Concave Mirrors.
(Configuration 1 and 2)

		Configuration 1 (weight=467lbs)	Configuration 2 (weight=343lbs)
Maximum Structural Deflection	RING	7.03×10^{-5}	13.92×10^{-5}
	6-60	7.74	14.71
	3-120	11.44	20.25
Optical Performance (RMS wave)	RING	0.282	0.646
	6-60	0.292	0.653
	3-120	0.883	1.473
Frequency (NASTRAN)	RING	492 Hz	360 Hz
	6-60	470	350
	3-120	362	281
Frequency (Closed-form)	RING	476 Hz	340 Hz
	6-60	455	330
	3-120	375	280

Table 5. The First Three Lowest Natural Frequencies for 40 inch Single Arch Mirrors

	Mode	RING	6-60	3-120
Double Concave (Configuration 1)	1	435 Hz	430 Hz	424 Hz
	2	930	810	442
	3	1230	1170	933
Double Concave (Configuration 2)	1	556 Hz	550 Hz	541 Hz
	2	1080	900	574
	3	1510	1360	1080

Table 6. A Comparison Summary of Single Arch Mirrors. (Configuration 1 and 2)

		Configuration 1 (weight=135lbs)	Configuration 2 (weight=165lbs)
Maximum Structural Deflection	RING	8.32×10^{-5}	5.38×10^{-5}
	6-60	8.54	5.67
	3-120	8.89	6.16
Optical Performance (RMS wave)	RING	0.175	0.132
	6-60	0.170	0.130
	3-120	0.162	0.130
Frequency (NASTRAN)	RING	435 Hz	556 Hz
	6-60	430	550
	3-120	424	541
Frequency (Closed-form)	RING	438 Hz	545 Hz
	6-60	432	531
	3-120	424	509

Table 7. A Comparison Summary of Double Arch Mirrors for a Contoured Back Shape Equation of EQN 2-3.

		Support point Ratio (r/Ro) 0.50	0.60	0.70
Maximum Structural Deflection	RING	10.66×10^{-6}	3.26×10^{-6}	8.03×10^{-6}
	6-60	14.04	6.61	11.25
	3-120	27.04	21.06	25.33
Frequency (NASTRAN)	RING	1080 Hz	1110 Hz	1000 Hz
	6-60	1050	1080	980
	3-120	930	920	900
Frequency (Closed-form)	RING	1220 Hz	2210 Hz	1410 Hz
	6-60	1070	1550	1190
	3-120	770	870	790

Table 8. A Comparison Summary of Double Arch Mirrors for a Ring Support at r/Ro=0.50.

	Contoured Back Shape Equation		
	EQN 2-3	EQN 4-5	EQN 6-7
Maximum Structural Deflection	10.66×10^{-6}	12.02×10^{-6}	11.52×10^{-6}
Frequency (NASTRAN)	1080 Hz	950 Hz	1030 Hz
Frequency (Closed-form)	1220 Hz	1150 Hz	1180 Hz

Table 9. A Comparison in Frequencies for Various Mirror Shapes.

	$\frac{r}{Ro}$	RING	6-60	3-120
Double Concave (Configuration 1)	1.00	1.00	0.96	0.74
Double Concave (Configuration 2)	1.00	1.00	0.97	0.78
Single Arch (Configuration 1)	0.15	1.00	0.98	0.96
Single Arch (Configuration 2)	0.20	1.00	0.97	0.95
Double Arch (EQN 2-3)	0.50	1.00	0.97	0.86
	0.60	1.00	0.97	0.83
	0.70	1.00	0.98	0.90

Table 10. Maximum Deflections of 40 inch SXA Flat Mirrors

unit = micro inches

D/t Ratio	Support System	Theory*	Axisym	Plate no Shear	Plate w/Shear	Solid
25	RING	265.63	270.20	271.58	273.51	270.13
	6-60	-	-	293.36	303.85	298.47
	3-120	485.16	-	488.48	515.59	508.58
16	RING	108.80	114.00	111.23	113.17	112.22
	6-60	-	-	120.18	127.94	128.88
	3-120	198.72	-	200.08	219.04	221.09
8	RING	27.20	30.57	27.81	29.74	30.66
	6-60	-	-	30.04	36.10	45.75
	3-120	49.68	-	50.02	63.61	82.66
4	RING	6.80	11.22	6.95	8.89	11.83
	6-60	-	-	7.51	12.97	35.96
	3-120	12.42	-	12.51	24.05	69.67

Table 11. Maximum Deflections of Contoured Back Mirrors

unit = micro inches

SHAPE	MODEL	RING	6-60	3-120
SINGLE ARCH	PLATE	66.83	67.16	67.80
	SOLID	44.44	48.70	54.60
DOUBLE ARCH	PLATE	9.73	11.57	24.08
	SOLID	7.57	11.68	23.18
	AXISY	7.52	-	-

Table 12. Optical performance analyses of Contoured Back Mirrors

unit = RMS wave

SHAPE	MODEL	RING	6-60	3-120
SINGLE ARCH	PLATE	0.186	0.186	0.186
	SOLID	0.027	0.027	0.025
DOUBLE ARCH	PLATE	0.014	0.028	0.274
	SOLID	0.004	0.009	0.166